Broadband Waveguide

CNF Project Number: 212612

Principal Investigator(s): Gregory David Fuchs

User(s): Srishti Pal, Qin Xu

Affiliation(s): Department of Applied Physics & Engineering and Department of Physics, Cornell University Primary Source(s) of Research Funding: Department of Energy (DOE) and Center for Molecular Quantum Transduction (CMQT)

Contact: gdf9@cornell.edu, sp2253@cornell.edu, qx85@cornell.edu

Research Group Website: https://fuchs.research.engineering.cornell.edu/

Primary CNF Tools Used: AJA Sputter Deposition, Heidelberg Mask Writer - DWL2000, GCA 6300 DSW 5X g-line Wafer Stepper, YES Asher, P7 Profilometer, Zeiss Supra SEM, Nabity Nanometer Pattern Generator System (NPGS), Dicing Saw - DISCO, Westbond 7400A Ultrasonic Wire Bonder.

Abstract:

We fabricate a broadband waveguide to test the magnetic properties of a low loss ferrimagnet vanadium tetracyanoethylene (V[TCNE]x) at cryogenic temperatures. We find that, in the temperature range between 0.44 K to 68.6 K, the linewidth of our V[TCNE] x sample increases with decreasing temperature. Below 0.44K, the resonance magnetic field decreases with decreasing temperature. These results are informative for the future applications of V[TCNE]x.

Summary of Research:

This research focuses on exploring exotic low-temperature broadband FMR response of the low-loss organic ferrimagnet V[TCNE]x.

The basic steps for patterning our broadband waveguide using photolithography are shown in Figure 1(a). First, we coat clean (with acetone followed by IPA) sapphire wafers with bilayer of LOR5A and S1813. The resist coated wafer is then exposed in 5X g-line Wafer Stepper to be patterned with the design written on a photomask using Heidelberg Mask Writer-DWL2000. The developed resist (in AZ726MIF) is descummed in YES Asher followed by deposition of 225 nm thick Ti/Cu/Pt tri-layer in the AJA sputter deposition tool. Finally, we lift-off the metal using 1165 and then dice the wafer using Dicing Saw-DISCO. For the magnon sub-system, we use the low-loss organic ferrimagnet V[TCNE]x with a low Gilbert damping $\alpha \sim 10-4$ offering long magnon lifetime and thus low Km. Using e-beam lithography in Nabity Nanometer Pattern Generator System (NPGS) connected to Zeiss Supra SEM, we pattern a 36 µm wide and 2 mm long bar on the 40 µm wide and 2 mm long central wire of the broadband chip using the steps shown in Figure 1(b). We then ship the exposed broadband chips to our collaborators in Ohio

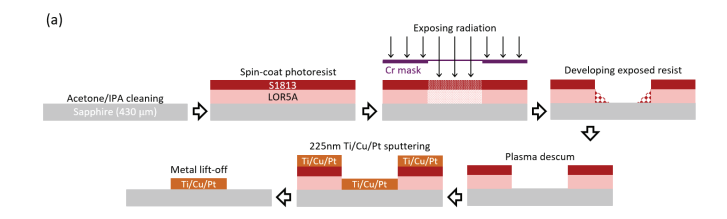


Figure 1: Process flow for (a) patterning the broadband chips with Ti/Cu/Pt tri-layer, and (b) e-beam patterning for V[TCNE]x deposition.

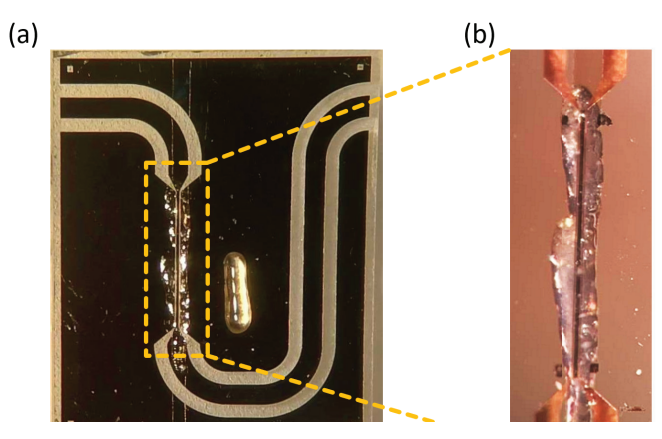


Figure 2: (a) Microscope image of broadband chip with patterned V[TCNE]x, ALD encapsulation, and protective grease layer. (b) Magnified microscope image of the region marked with yellow dashed rectangle in (a).

State University for V[TCNE]x growth and liftoff.

The V[TCNE]x is then encapsulated by ALD Alumina by our collaborators in Northwestern University to prevent degradation from air exposure and then sent back to us for measurement. We finally applied an additional layer of cryogenic grease for further protection of the V[TCNE]x film as shown in Figure 2.

For the FMR measurement setup, we first put the sample into a dilution refrigerator which has a base plate temperature of 15 mK. The broadband waveguide

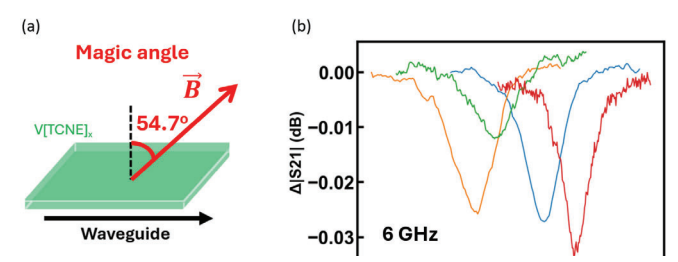


Figure 3: (a) Measurement setup scheme showing the orientation of the external field relative to the waveguide and the V[TCNE]x film. The external field is at 54.7•from the film normal of the V[TCNE]x film. (b) Microwave transmission spectrum vs the external magnetic field magnitude when the microwave frequency is 6 GHz. We can see the dip of the FMR resonance at different microwave excitation powers or temperatures. The 4 dips from left to right are obtained at -68 dBm microwave power at the sample in the dilution fridge; -58 dBm in the dilution fridge; -48 dBm in the dilution fridge; and -83 dBm at 0.44 K in the He-3 cryostat.

is connected to a vector network analyzer for the microwave transmission measurement. As shown in Figure 3(a), the external magnetic field is applied at 54.7• from the film normal (the magic angle) of the V[TCNE]x film. In this geometry, the inhomogeneous

linewidth caused by the length of the V[TCNE]x is minimized.

Figure 3(b) shows the 6 GHz microwave transmission magnitude vs the external magnetic field magnitude at different driving powers. When the V[TCNE]x's Larmor frequency matches 6 GHz, it will absorb some of the microwave energy, thus causing a dip in the transmission spectrum. The 3 dips on the left are the

transmission spectrums when the microwave powers at the sample are -68 dBm, -58 dBm and -48 dBm

respectively. The dip shifts to a higher magnetic field when the excitation power is higher, which is later shown to be caused by the heating of the V[TCNE] x. In other words, the dip shifts to a higher magnetic field when the sample temperature is higher. Note that this shifting happens at all directions of the external magnetic field, which rules out temperature dependent changes in magnetic anisotropy.

Then, the sample chip was put into a He-3 cryostat that has a tunable temperature between 0.44 K and 70 K. The rightmost dip in figure 3(b) is got when the sample space temperature is 0.44 K with -83 excitation power, which proves that the resonance field shift is caused by the raising temperature. Figure 4 shows the linewidth of the V[TCNE]x at 6 GHz and 14 GHz. It shows that the linewidth of V[TCNE]x increases with decreasing temperature. Also, most of the linewidth is due to frequency-independent broadening.

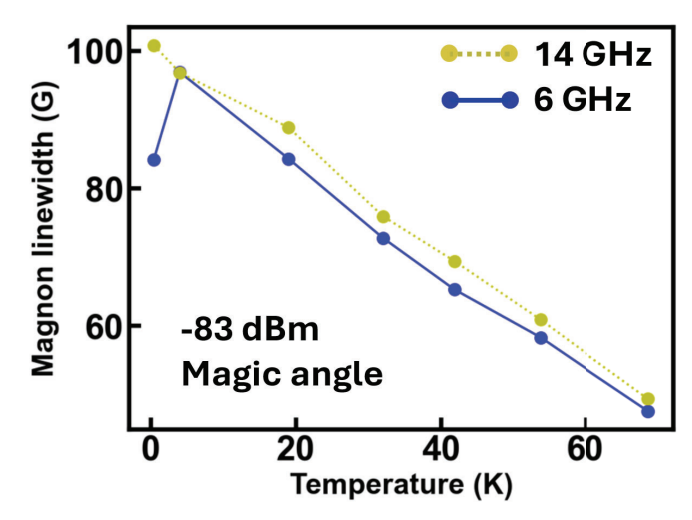


Figure 4: FMR linewidth of V[TCNE]x at 6 GHz and 14 GHz at different temperatures. The microwave power is -83 dBm.

Conclusions and Future Steps:

We fabricate a microwave frequency waveguide chip and use it to measure the broadband FMR of V[TCNE] x at cryogenic temperatures. We see an increase in FMR linewidth from 68.6 K to 0.44 K and a shift in resonance magnetic field vs temperature below 0.44K. More experiments are needed to fully characterize the sources of the observed linewidth and frequency changes.

References:

- [1] H. F. H. Cheung, M. Chilcote, H. Yusuf, D. S. Cormode, Y. Shi, S. Kurfman, A. Franson, M. E. Flatté, E. Johnston-Halperin, and G. D. Fuchs, "Raman Spectroscopy and Aging of the Low-Loss Ferrimagnet Vanadium Tetracyanoethylene", The Journal of Physical Chemistry C 125, 20380 (2021).
- [2] Q. Xu, H. F. H. Cheung, D. S. Cormode, T. O. Puel, S. Pal, H. Yusuf, M. Chilcote, M. E. Flatté, E. Johnston-Halperin, and G. D. Fuchs, "Strong Photon-Magnon Coupling Using a Lithographically Defined Organic Ferrimagnet", Advanced Science 11, 2310032 (2024).